Purification of Volatile Organic Compounds in Channeled Ventilation Pipes at the Sysav Water Treatment Plant for Hazardous Waste

by

Erik Wiktorsson

Department of Chemical Engineering

Lund University

March 2022

Supervisor: Christian Hulteberg
Co-supervisor: Alafarid Dabas
Examiner: Ola Wallberg

Postal address
P.O. Box 124
SE-221 00 Lund, Sweden
Web address
www.chemeng.lth.se

Visiting address
Getingevägen 60

Telephone
+46 46-222 82 85
+46 46-222 00 00
Telefax
+46 46-222 45 26

Acknowledgement

I would like to thank my supervisor Christian Hulteberg at LTH for being an invaluable source of knowledge and support, and Alafarid Dabas at Sysav for his professional guidance and always positive attitude around the plant. It has been a truly rewarding experience.

Lund, May 2022

Erik Wiktorsson

Abstract

Several channeled emissions at the Sysav water treatment plant for hazardous waste as of December 2021 exceed permitted levels of unknown volatile organic compounds (VOCs) stated in the European Parliament councils' directives 2010/75/EU.

A range of possible treatment methods are briefly discussed before zeolite adsorption, and thermal regeneration followed by catalytic combustion is decided to be the method of greatest feasibility and is the subject of further investigation.

The zeolite suggested is faujasite zeolite of high silica content (Faujasite (Y) HY901) due to its large pore sizes and hydrophobic nature.

The catalyst suggested is a manganese oxide (Mn_3O_4) due to its lower cost than that of noble-metal catalysts, as catalyst poisons present may result in rapid deterioration of the catalyst.

A process flow chart is presented, which includes two parallel zeolite beds that operate in shifts, followed by catalytic combustion. Heat recovery is possible, and a heat exchanger is implemented after combustion to heat the regenerative air flow.

The process is modeled as steady-state, and results include general dimensions as well as capital and operational costs. Calculated with the software EconExpert, the resulting capital costs as estimated are 12,-800,000 SEK. Operational costs are approximately 200,-000 SEK/year after two years.

For future work, it is of crucial importance to determine what VOCs are present for accurate modeling and predictions.

Sammanfattning

Flera utsläppspunkter vid Sysavs vattenreningsverk för farligt avfall överstiger vid tillfälle december 2021 de tillåtna utsläppsnivåer av okända flyktiga organiska föreningar (VOCs) som anges i Europaparlamentets direktiv 2010/75/EU.

Ett par möjliga reningsmetoder diskuteras kort innan zeolitadsorption och termisk regenerering följt av katalytisk förbränning beslutas vara den metod som har bäst förutsättningar att genomdrivas och är föremål för närmare granskning i rapporten.

Zeoliten som föreslås är faujasitzeolit av hög kiselhalt (Faujasit (Y) HY901) på grund av dess stora porstorlekar och hydrofoba natur.

Den föreslagna katalysatorn är en manganoxid (Mn_3O_4) på grund av dess lägre kostnad jämfört med den för ädelmetallkatalysatorer, då närvarande katalysatorgifter kan resultera i påskyndad förgiftning av katalysatorn.

Ett processflödesschema presenteras där 2 parallella zeolitbäddar arbetar i skift, följt av katalytisk förbränning. Värmeåtervinning är möjlig och en värmeväxlare implementeras efter förbränning för att värma upp det regenerativa luftflödet.

Processen är modellerad som steady-state och resultaten inkluderar dimensioner samt kapital- och driftskostnader. Resulterande kapitalkostnader är 12 800 000 kr. Driftskostnaderna är cirka 200 000 kr/år efter 2 år.

För framtida arbete är det av avgörande betydelse att fastställa vilka VOCs som finns närvarande för korrekt modellering och förutsägelser.

Table of Contents

1. Introduction

In Chapter 1, some basic understanding of the report is presented. The real-life problem at hand and the aims, implementations and limitations of the project are here briefly discussed.

1.1. Background

During the fall in 2021 at the Sysav water treatment plant for hazardous waste, a new purification step involving flotation is installed and put into operation. This means the plant is carrying out physical-chemical purification of waste and thus is governed by the Industrial Emissions Directive (classified as an IED-plant).

Due to this new classification, the plant must meet the conditions that apply for such stated in the Best Available Technology - Associated Emission Levels (BAT-AEL). The plant must also fulfill the remaining conditions in the BAT-conclusions for waste treatment, in agreement with the European Parliament and the councils' directives 2010/75/EU.

In the BAT-AEL, channeled emissions are defined as follows:

Emissions of pollutants into the environment through any kind of duct, pipe, stack, etc. This also includes emissions from open-top biofilters.

To check the status of the plant in relation to the given values in the BAT-AEL, an extended scheme of analysis has been introduced since the month of May 2021 regarding the parameters stated in the BAT-conclusions. A measurement on channeled emissions to air has also been carried out. The measurement shows exceeding concentrations of *total volatile organic compounds* (TVOC/VOC) in 3 out of 5 points of measure. The highest allowed concentration of TVOC in IED-plants is 20 mg/Nm^3, however, the highest concentration measured in May 2021 was found to reach closer to 400 mg/Nm^3.

Any proposed installations must be in place and in operation by the latest of August 22nd 2022.

1.2. Aim

The aim of this thesis is to conclude and propose the most viable solution for the water treatment plant to reach TVOC goal values within the given time span, both in terms of environmental as well as economic efficiency.

1.3. Implementation

With available BAT-documents it is possible to narrow down some techniques that are of reasonable interest for further investigation. These will then be evaluated in terms of technical efficiency, cost and time of installment, as well as costs of operation, and with these results give qualified recommendations on implementations.

1.4. Limitations

Due to the broad task to investigate the best technical solution for a gas stream of unknown and varying VOCs, this report will be limited to a few common and plausible VOCs, and the possibility to remove these with a technical solution seems fit for the Sysav water treatment plant for hazardous waste.

2. Conditions at the Sysav Water Treatment Plant for Hazardous Waste

In Chapter 2, the conditions at the plant are presented as-is. A list of plausible VOCs that are of interest for further studies is also presented in Section 2.2.

2.1. Volumetric Flows and Concentrations

ILEMA Miljöanalys AB was hired to measure a variety of emission concentrations at the Sysav water treatment plant for hazardous waste, including VOCs. A process flow diagram in Swedish of the water treatment plant is presented in Figure 1 below. The red flows mark the newly installed flotation steps. Denoted volumetric flows are liquid and not to be confused with VOC laden air.

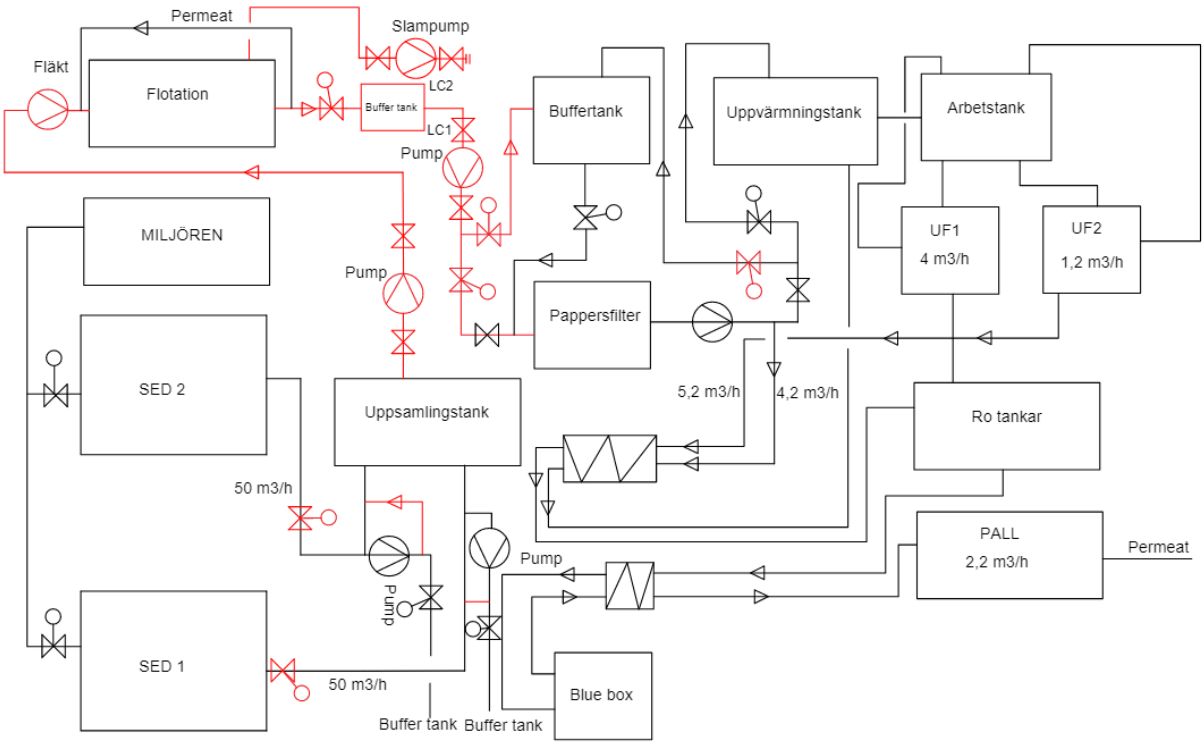

Figure 1: The process flow diagram of the Sysav water treatment plant (in Swedish).
Fällningen = Precipitation
PALL = RO Membrane
Pappersfilter = Paper filter (with gathered streams)
Sludge container: After "Slampump", not shown here

The first set of measurements was conducted on the 19th of May 2021, before the installation of the flotation step. The second set of measurements was conducted on the 30th of November 2021, after the installation of the flotation step.

VEAB was also hired on two occasions to measure some remaining volumetric flows to complete the picture after the flotation step had been installed, on the 9th of November 2021 and the 1st of December 2021.

Measured points that exceeded permitted TVOC levels at any occasion are here listed below to serve as a basis to later dimension any purposed solution.

Clarification regarding the missing flows at the Precipitation:

The precipitation step does have a channeled emission and thus falls under the conditions that apply for such stated in the BAT-AEL. However, this step is rarely in use. Measurements were still carried out by ILEMA AB by measuring close to the precipitation step but open to the atmosphere and not in a vent.

For the purpose of any mass balance, this will have little impact, as concentrations are low and no air is actively vented out.

Clarification regarding the disregarded flow at the RO Membrane

The volumetric flow at the RO membrane was measured both by ILEMA AB and VEAB. To avoid later under dimensioning, the lesser flow is disregarded.

Table 1 Measured volumetric flows and VOC concentrations.

Point of measurement / **Property measured**	**Precipitation**	**RO Membrane**	**Paper filter (with gathered streams)**	**Sludge container**
TVOC-concentration [mg/m³ntg] **By: ILEMA AB**	25.8* 8.97**	392* 345**	125* 72**	-* 80**
Total volumetric flow (dry gas) [m³ntg/h]	-	129†, * 110†, x, ** 414‡, **	1120†, * 5520†, **	-* 605‡, **
Resulting TVOC emissions [kg/day]	-	1.21* 3.43**	3.36* 9.54**	-* 1.16**
Total summed resulting TVOC emissions [kg/day]	4.57* 14.13**			
Resulting combined total volumetric flow [m³ntg/h]	1249* 6539**			
Resulting combined TVOC-concentration [mg/m³ntg]	153* 90**			
Resulting combined TVOC-concentration assuming a molar weight of 65g/mol and ambient conditions [ppm]	58.7* 34.5**			

** = Measurement before installed flotation step*
*** = Measurement after installed flotation step*
† = By: ILEMA AB
‡ = By: VEAB
x = Disregarded

2.2. Listed VOCs In This Study

The VOCs subject for further studies is determined to cover some common VOCs with a range of different molecular characteristics, such as polarity, functional groups, and aromatics, as well as for which one's data was available in literature and studies. The diameter is taken as the Lennard-Jones parameter σ in the cases it was found, and the spherical diameter is roughly calculated assuming the molecules to be spherical and neglecting any interaction forces, calculations in Appendix A.1. These VOCs are presented with some general characteristics in Table 2 below.

Table 2: VOCs assumed for further studies.

VOC	**Diameter (Å)**	**Boiling point (°C)**	**Relevant uses**	**Molecule**
Acetone, C_3H_6O	4.76* 5.7**	56	Solvent Cleaning agent	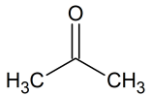
Butanone, C_4H_6O	6.6**	80	Solvent	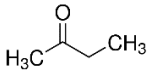
Ethanol, C_2H_5OH	4.34* 6.2**	78	Solvent	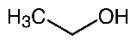
Isopropanol, C_3H_8O	6.2**	83	Solvent	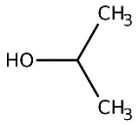
Methanol, CH_3OH	5.0**	65	Solvent Building block chemical	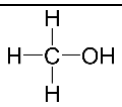
Hexane, C_6H_{14}	5.92* 7.5**	69	Solvent	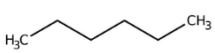
Toluene, $C_6H_5CH_3$	5.64* 7.0**	110	Solvent	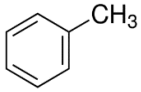

** = Lennard-Jones parameter σ (Wilhelm and Battino, 1971)*

*** = Estimated spherical diameter*

3. VOC Removal Methods

There are many developed technologies in the field of air purification and VOC removal. They all have their advantages and disadvantages and are of varying applicability for different purposes and industries. In Chapter 3, some of the most common solutions are briefly described to lay the foundation for the choice of technology subject to further investigation.

3.1. Method of Removal Criteria

At the Sysav water treatment plant for hazardous waste, the VOC laden streams of interest are of a wide variety of qualitatively unknown VOCs at relatively high concentrations. Some criteria that should be fulfilled are presented as bullet points here below.

- To reach sufficiently low acceptable VOC concentration levels, the method must be efficient to a degree of at least >90%.
- As the individual species of the VOCs are unknown, the method must be robust and reliable for a wide variety of such.
- Some methods may be highly efficient but too costly, either in capital or operational costs, or both. The method should be cost reasonable.
- To eliminate the need for further processing of for example filter media used, it is beneficial if the method is destructive to the VOCs on site.
- The method should be safe and overall reasonable.

3.2. Common Technical Solutions for VOC Removal

In Section 3.2, some of the more (and maybe less) common solutions are presented and discussed as possible solutions for the plant.

3.2.1. Thermal Incineration

A simple yet effective way to treat VOC emissions is to incinerate them in a combustion chamber. The VOCs enter the chamber where auxiliary fuels incinerate the VOCs. Most hydrocarbons ignite at temperatures below 700K, but by bringing the temperatures up to about 950K, a 99.99% removal rate can be achieved (O'Reilly, 1998). A generalized reaction can be represented as VOC → CO → CO_2, with water and potential byproducts formed depending on the composition of incoming gases.

There are many cleverly designed configurations for the combustion chamber, two common ones being the Recuperative Thermal Oxidizer and the Regenerative Thermal Oxidizer. Both these designs are designed as inherent heat exchangers to reduce fuel usage, which often becomes a costly factor. This cost can be further reduced with higher VOC concentrations, as the VOCs will become more autothermal.

3.2.2. Catalytic Incineration

Catalytic incineration much resembles the uncatalyzed thermal incineration but incorporates a catalyst, as the name suggests. Typical catalysts for VOC incineration include precious metals such as platinum and palladium. For chlorinated compounds, various metal oxides can be used (Kosusko & Nunez 1990).

The presence of a catalyst allows for the incineration to occur often at several hundred degrees lower than otherwise possible, thus lowering fuel costs. However, the process gas to be cleaned should be properly investigated so that no catalyst poisons or inhibitors are present that could degrade the catalyst. If a specific catalyst poison is prominent, steps may be taken to remove the contaminant more specifically before reaching the catalyst.

3.2.3. Carbon Adsorption

Activated carbon is a highly porous processed carbon material with a massive internal surface area, and adsorption via activated carbon is a widely used non-destructive technique in many sectors. The activated carbon acts as a filter until it is saturated and is then disposed of or more often, steamed for regeneration. Activated carbons come in many forms and shapes and can be further surface modified to meet more specific needs. They can often be a very useful and economically viable solution for VOC emissions.

There are, however, some key drawbacks that should be addressed and considered before employing a carbon filter solution for VOC removal.

One potential drawback with activated carbon is its low ignition point in combination with the exothermic nature of adsorption. This should be further emphasized when certain VOCs such as ketones and aldehydes are to be adsorbed, as they may cause highly exothermic reactions within the carbon bed, potentially causing a carbon bed fire (Kienle et al., 1994). This might become also become a risk during potential thermal regeneration of the bed.

Commonly used industrial solvents often contain some amounts hydrocarbons with high boiling points. This becomes a problem when using activated carbon as high temperatures are required during regeneration of these, which may lead to more rapid carbon degradation (Chihara et al., 1981).

Another factor to consider is the humidity of the gas. Activated carbon retains water, which lowers the overall performance of the carbon. The retained water within the carbon also increases the amount of energy required during regeneration due to the high enthalpies of evaporation. A humid gaseous flow will thus decrease the lifetime of the carbon filter and increase operating costs.

3.2.4. Zeolite Adsorption

Zeolite adsorption works by the same mechanism as carbon adsorption, but since the zeolite is an oxide, it is much more heat resistant and durable. This allows for long going thermal swing adsorption, where the large flow of cool polluted air is passed through the zeolites. When the zeolites are saturated, the inflow is switched to one of hot air in much smaller volumetric quantities and passed through the saturated zeolites. This desorbs the VOCs, and a now concentrated air flow can easily be burned off, as the VOCs themselves are flammable.

The risk of a bed fire is also eliminated as the zeolites will not burn; thus, zeolite beds are inherently safer than carbon beds. Large hydrocarbons with high boiling points that get stuck in the bed can often be torched off if necessary.

The major drawback with a zeolite adsorption system tends to be capital costs, but this would have to be weighed to the lower operating costs due to the longer lifespan and recoverability of the zeolites compared to the carbon adsorption alternative.

3.2.5. Scrubber Absorption

Scrubber absorption can be a highly selective method of VOC removal. Scrubber absorption is typically used in in cases of steady streams and well defined and often valuable emission VOCs to be recovered, where a suitable solvent can be chosen for absorption and desorption (Saito, 2004).

3.2.6. Biofilter

Biofiltration for VOC removal is a method where contaminated air is passed through a packed column of enrichment culture. The culture can be derived from compost and feeds upon the VOC pollutants with carbon dioxide and water as the main end products. Biofilters may operate either in continuous or somewhat intermediate processes, although preferably continuous. The removal efficiency of the biofilter increases with time and may stabilize first after some 60-90 days.

Reports of biofilter VOC removal efficiency vary vastly depending on loading quantity and quality.

A laboratory-scale study limited to 5 VOCs commonly found in the paint industry showed very promising results of <99% (Moe & Qi, 2005).

A larger study, applying a biofilter first after passing the polluted air through a spraying tower, focused on a wider variety of 50 VOCs commonly found in the textile dying industry divided into four groups: nitrogen- and oxygen-containing compounds (NAOCCs), aliphatic hydrocarbons (AIHs), aromatic hydrocarbons (AHs), and halogenated hydrocarbons (HHs). Average removal efficiencies for the groups were 66.7%, 67.9%, 11.7% and 52.1%, respectively (Liang et al., 2020).

3.2.7. UV Photocatalyst

In UV photocatalytic destruction of VOCs, the semi-conductor titanium dioxide (TiO_2) is typically used. TiO_2 has a bandgap of 3.2 eV and is activated by UV light at a wavelength λ = 387 nm. The excited electrons react with oxygen in the air to form superoxide radical anions $O_2^{\bullet-}$, and the formed electron holes react with water in the air to form hydroxyl radicals $^{\bullet}OH$. Both these highly reactive radicals react with VOCs present in the air to form carbon dioxide and water (Mull et al., 2017).

Whilst the technique may be a promising emerging technique, it is as today typically employed as an air-purifying system for indoor work environments rather than an industrial VOC removal technique (Huang et al., 2016).

3.2.8. Corona Destruction

Corona destruction is a destructive technique in which electrons are generated by inducing electric fields.

One design is to use a packed bed reactor with pellets of a high dielectric, ferroelectric material and apply an alternating current. This creates micro electric fields in the interstitial spaces between the pellets called corona sites. Another design is a wire-in-tube reactor, where high-voltage pulses are passed through the tube at high frequencies. Electrons are generated at the corona sites and gain kinetic energy until they may undergo an inelastic collision with a particle nearby, transferring its kinetic energy to the target species causing ionization, dissociation, or excitation. These effects can either be destructive in themselves or initiate a destructive series of reactions for the target species (Kariher et al., 1993).

Corona destruction has some key advantages in regards to low operating costs, insensitivity to poisoning, high performance even at very low concentrations and the ability to operate under ambient conditions.

Unfortunately, corona destruction does not perform equally well for all types of VOCs.

When Kariher et al. conducted their experiments in 1993, an inlet stream of varying VOCs at concentrations of 100 ppmv was passed through the packed bed design with barium titanate as ferroelectric material. Destructive removal efficiency for benzene was determined to be close to 100%, but only 15% for that of methane.

Thus, corona destruction may be a suitable option only when emission contents are well defined.

3.3. Suggested Method

The methods subject for further studies are set to be thermal swing adsorption with zeolites, followed by catalytic incineration.

The choice of zeolite is based on the robustness and adsorption efficiency of an accurately selected zeolite material, in combination with the inherent safety that comes with the zeolites non-flammability compared to that of active carbon.

With zeolite adsorption naturally follows desorption and incineration, where a catalyst often can be favorably applied.

4. Suggested Method

The suggested method presented in the last section of Chapter 3 is here further discussed and investigated.

4.1. Zeolites

In Section 4.1, zeolites and various crystal factors affecting their properties are discussed. A specific zeolite is then suggested based on experimental results from a previous study.

4.1.1. Briefly About Zeolites

Zeolitic materials, either natural or synthetic, are crystalline aluminosilicates uniformly sized and shaped micropores of windows, cages, and supercages (CATC, 1998). These micropores can adsorb molecules small enough to fit within them whilst excluding ones that are too large to fit. The aluminosilicate framework mainly consists of SiO_2 interspersed with AlO_2^-, where loosely held cations sit within cavities to preserve overall electroneutrality. Some cations are amenable to cation exchange, and the zeolite can readily reversibly adsorb polar molecules (Maesen, 2007).

The properties of the zeolites are essentially determined by their crystalline structures. In the case of adsorption, selectivity depends upon pore sizes, as capacity depends upon accessible void volume. The hydrophobicity of the zeolite is also important and can be increased by increasing the Al/Si-ratio. Thus, determining structural requirements becomes crucial when designing the zeolite adsorption bed.

As of July 2021, there were 255 registered zeolite framework types with the Structure Commission of the International Zeolite Association, and only 17 of these are of commercial value. Out of the 17 commercially valuable structures left, the 4 hydrophobic MFI-, FAU-, MOR- and BEA-type silica zeolite framework types are typically of interest for VOC removal (Maesen, 2007, McCusker & Baerlocher, 2007).

These three-lettered codes for various zeolite framework types are clearly defined and differ from the zeolite structure. Zeolites commonly share the feature of being a 3-dimensional, 4-connected framework structure connected to a TO_4 tetrahedra, where the T is a tetrahedrally coordinated cation. A zeolite framework type does not consider chemical composition, but rather structural features such as cages, channels, chains and sheets are often characteristic of a zeolite framework type, hence why it is defined.

It should be noted that even though the structure and framework type of the zeolite both play large roles in overall resulting properties, neither completely defines the chemical composition, which plays an important role as well. For example, a composition of aluminosilicate will be an anion balanced with a cation, whereas aluminophosphate will be electroneutral as is. This cation may partly block or disrupt the pores of the framework, changing its properties. Thus, the chemical composition should be considered as well (McCusker & Baerlocher, 2007).

4.1.2. Crystal Factors Affecting Zeolite VOC Adsorption Abilities

The nature of the zeolite crystal determines its sorptive abilities. Some key factors are here briefly mentioned and how they affect the adsorption.

4.1.2.1. Crystal Structure

The zeolite crystal structure determines a large portion of its properties as it makes up and dimensions the channels of the zeolite. The crystal structure of a zeolite can be determined by oxygen numbers, meaning the number of T-atoms participating in the rings of the crystal. The dimensions and geometries of the resulting channels determine what molecules may be adsorbed. Larger channels allow for higher adsorption capacity as larger molecules may enter.

4.1.2.2. Si/Al Ratio

An increasing ratio between silicon and aluminum results in an increasingly hydrophobic character of the zeolite. In some zeolite applications, a hydrophilic surface may be desired. However, in many cases of gas purification, humidity soon becomes an issue with hydrophilic zeolites as water molecules inhibit the vacancies.

4.1.2.3. Pore Volume

The volume of the micropores ($d < 2nm$) of the zeolite is not correlated to the amount VOC adsorbed, as the volume of the mesopores ($2nm < d < 50nm$) is positively correlated to the amount VOC adsorbed (Kim and Ahn, 2011).

4.2.2.4. Pore Structure

The pore structure may affect the adsorption by mechanical means. For example, a zeolite may have pores with long narrow necks which may lower adsorption rates.

4.1.3. Suggested Zeolite

In section 4.1.3., the VOC adsorptive abilities of a variety of zeolites have been previously experimentally evaluated, and the results will lay the foundation for any zeolite later suggested.

4.1.3.1. Experimental Basis

A thorough study of 6 selected zeolites' performances in treating a model VOC laden helium gas was presented by Ki-Joong Kim and Ho-Geun Ahn in 2011 (Kim and Ahn, 2011). As the model VOC gas of their study much resembles the list of plausible VOCs at the Sysav water treatment plant for hazardous waste, their experimental results will be assumed to be a reliable indicator.

4.1.3.1.1. Investigated Zeolites and VOCs

The list of investigated zeolites is reproduced in part below in Table 3, and the contents and composition of the used model VOC gas in Table 4.

Table 3: Commercially available zeolites investigated by Ki-Joong Kim and Ho-Geun Ahn in 2011.

Zeolites	**Product and vendor**	**Symbol**	**Si/Al ratio**
Mordenite	Z-HM10(2) (JRC)	HMOR	10.2
	TSZ-640NAA (Tosoh)	NaMOR	19.0
Faujasite (Y)	Z-HY5.6(2) (JRC)	HY5.6	5.6
	Z-HY4.8 (JRC)	HY4.8	4.8
	HY901 (Zeolyst)	HY901	80.0
Faujasite (X)	Molecular sieve 13X (Aldrich)	MS13X	<1.5

Table 4: Contents and composition of used model VOC gas used by Ki-Joong Kim and Ho-Geun Ahn in 2011.

Aromatics	**Mol.%**	**Alcohols**	**Mol.%**	**Ketone**	**Mol.%**
Benzene	3.58	Methanol	2.88	Methylethylketone	4.99
Toluene	5.90	Ethanol	4.42		
o-xylene	0.97	Iso-propanol	9.94		
m-xylene	0.95				
p-xylene	1.80				

4.1.3.1.2. Summarized Results

The adsorption capacities of the faujasites were superior to those of the mordenites, with faujasite (Y) HY901 and faujasite (X) MS13X showing 1st and 2nd longest breakthrough times, respectively. These adsorption capacities have been calculated and are presented in Appendix A.2 together with the raw data of the breakthrough times.

It can be shown that the connecting 12-member oxygen rings of the faujasite type framework provide for a 13 Å free diameter, whereas the connecting 12- to 8-member oxygen rings of the mordenite only provide for 6.8 Å, hence the higher adsorption capacities of the faujasites.

Faujasite (Y) HY901 is a high silica zeolite (Al/Si = 80), as faujasite (X) MS13X is a low silica zeolite (Al/Si < 1.5). This difference seemed irrelevant to the absorbance capacities of this study.

4.1.3.2. Suggested Zeolite

Even though the higher Si/Al ratio did not seem to diminish the absorbance capacity in this study, the VOC laden air at the Sysav water treatment plant will be of higher water content.

Thus, to reduce the energy requirements of evaporating water trapped within the zeolite, the applied zeolite should be a faujasite zeolite of high silica content.

4.2. Catalysts

To effectively incinerate the concentrated VOC laden air stream and fully convert its contents to CO_2 and water, catalytic incineration is widely applied industrially as an effective and economically feasible method. By operating at relatively low temperatures and controlled conditions, catalytic incineration also prohibits the formation of undesired byproducts such as dioxins and NO_x (Liotta, 2010). VOC incineration catalysts are typically some noble metal supported on an aluminum oxide or silicone oxide, where the catalytic properties arises from the partially filled d-subshells of the noble metal.

The catalyst could be employed in various ways, mainly as a fixed-bed catalytic reactor or a flow-through membrane reactor. The catalyst should be chosen to effectively eliminate the specific VOCs of the air stream, and different catalysts could be stacked in layers or placed in series if they are not sufficiently effective for the individual VOCs by themselves. Some key factors when choosing a catalyst are cost, efficiency, thermal stability, and catalyst poisons present. If high levels of a catalyst poison are found, pretreatment could be necessary if possible to prolong the lifespan of an expensive catalyst.

4.2.1. Catalyst Poisons

Catalyst poisoning is the phenomenon of partial or total deactivation of a catalyst by a chemical compound. Most often, the mechanism of the poisoning is a formed chemical bond between the catalyst and typically a polar or ionic compound, inhibiting the active site of the catalyst. The company ILEMA AB was hired to measure the amounts of some common catalyst poisons: sulfur, phosphorous, and halogens. The results are presented in Table 5 below.

Catalyst poisons are present only in small amounts and should not adsorb onto the hydrophobic zeolite bed. Thus, a catalyst bed can bed applied without being exhausted all too quickly.

Table 5: Catalyst poisons present at measured points.

Point of measurement / Property measured	Precipitation*	RO Membrane	Paper filter (with gathered streams)	Sludge container	Total
HCl [mg/m³ntg]	0.08	0.049	0.11	0.089	0.2480
HF [mg/m³ntg]	0.012	0.0019	0.0220	0.0099	0.0338
Phosphorous [mg/m³ntg]	<0.0025	0.0018	<0.0056	<0.0046	<0.0120
Total sulfur [mg/m³ntg]	<0.4	0.29	<0.42	<0.73	<1.4400

*Note 1: * = Disregarded and not added to the Total column since VOC-levels no longer surpass legal levels*

4.2.2. Possible Catalysts

In Section 4.2.2, two categories of catalysts are discussed; the noble metals and the non-noble metals. In section 4.2.3, the results of the discussions are weighed against each other, and a catalyst is finally suggested.

4.2.2.1. Pt, Pd and Rh Catalysts

These noble metals have been widely applied as catalysts in the abatement of VOCs despite their high costs due to their high specific activity, resistance to deactivation, and ability to be regenerated. Many factors affect these metals' catalytic abilities, such as the method of preparation, type of precursor, metal loading and particle size, and the nature of the support. Their performance also highly varies depending on the VOC nature, be it an alkane, alkene or aromatic. Industrially, the metals are typically supported on high-surface γ-Al_2O_3 powder and wash coated on either a ceramic (cordierite) or metallic (aluminum or stainless steel) monolith, with a channel density of no higher than 200-400 channels per square inch (cpsi) to reduce the pressure drop and to avoid clogging and coking (Liotta, 2010).

Among the three, it is the Pt/γ-Al_2O_3 catalyst that has been claimed to be most effective by several authors against a wide range of VOCs of different natures, such as n-hexane, methanol, n-butyl-amine, toluene, propane and propene, with the Rh/γ-Al_2O_3 catalyst showing greater conversion only for larger alkenes like hexene. The Pt catalyst, however, comes with the potential drawback of being greatly inhibited in the presence of carbon monoxide (Liotta, 2010). This effect may be combatted by the addition of a gold catalyst over a titanium oxide support Au/TiO_2, due to golds' high activity towards CO (Kozlova et al., 2004). It should be noted that full conversion of hexene, toluene and benzene may be achieved at relatively low temperatures by the Pt catalyst, even without the addition of Au/TiO_2 in the presence of CO.

It should further be noted that as of today the Rh catalyst is rendered practically useless due to its high costs.

4.2.2.2. Mn, Ce, Co, Cu and Fe Catalysts

Non-noble metal catalysts may compete with the noble metals on the basis of being much cheaper yet still being highly efficient and resistant to catalyst poisons. These properties have made many cheaper metals interesting for further studies, in particular Mn, Ce, Co, Cu and Fe. It is the manganese catalysts of different sorts that have shown the most continuously high performances regarding catalytic VOC incineration when benzene, toluene, ethanol, and ethyl acetate have been investigated (Zhu et al., 2015, Kima and Shim, 2010, Aguero et al., 2009).

4.2.3. Suggested Catalyst Bed

The task of predicting the best-suited catalyst bed for a stream of unknown VOCs simply is not possible. This is due to the highly varying efficiencies of different catalysts towards different VOCs, as well as synergistic and competing effects for the active sites of the catalyst amongst the VOCs. This is the subject of many studies, where seldom more than three different VOCs are tried at the same time at different ratios. To ensure sufficient combustive efficiency and catalyst lifespan, pilot-scale experiments must be carried out on site.

This study will further focus on a Mn_3O_4 catalyst in a pellet plug-flow reactor configuration, with an assumed catalyst efficiency of >99.9% with a catalyst capacity of 7500 m^3/h VOC laden air per m^3 catalyst at an operating temperature of 350 °C. This is because the Mn_3O_4 catalyst has shown very high conversion rates (>99.9%) for some VOCs at operational temperatures as low as 250 °C (Kima and Shim, 2010). To ensure sufficient conversion of VOCs outside this study, the actual operation temperature was elevated by 100 °C.

It is also the suggested catalyst on the basis of being much cheaper than its noble metal counterparts, which would prove economically reasonable if catalyst poisons would prove an issue.

4.3. Process Flow Chart and Zeolite/Catalyst Vessel Designs

After reviewing some zeolite-catalyst solutions, a process flow chart is suggested. It is equipped with two zeolite beds and one catalyst vessel, and incorporates some heat exchange. The suggested process is presented in full as a flow chart in Figure 2 below.

The blue streams represent the adsorptive stream. The VOC laden air is passed through a zeolite column (Bed 1), and VOCs are adsorbed before it exits the column as clean air.

The red streams represent the regenerative streams. Compressed air is passed through a heating coil (Heat Coil 2) to reach sufficient temperature for the VOCs to desorb from the zeolites (Bed 2). Compressed inert nitrogen is available on stand-by in case temperatures in the catalyst reach too high. The regenerative stream flows counter-current to the adsorptive stream. This is because of the concentration profile of the VOCs adsorbed within the zeolite column; the highest concentration is found where the adsorptive stream enters the column, and the lowest where it exists. Instead of pushing an intersecting plane of the highest concentration through the full column, the flow is reversed so that a smaller total amount of VOCs has to travel through the column during regeneration. After the VOCs are desorbed and concentrated, they are again sent through a second heating coil (Heat Coil 2) to reach sufficient temperature to be catalytically combusted (Catalytic Incineration). Heat is released upon combustion, quantitively depending on VOC specimen. This heat may be recycled with a heat exchanger (Heat Exchanger) to lessen operational heating costs.

The yellow and green streams are streams on stand-by for when the beds switch between adsorption and regeneration.

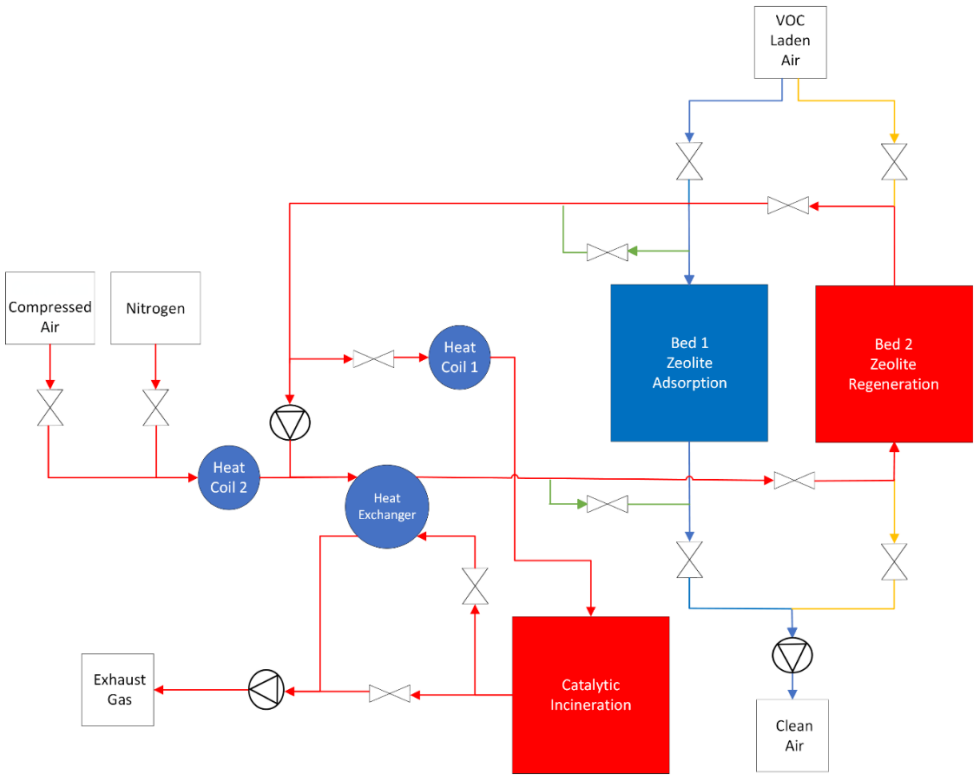

Figure 2: Flow chart of the suggested method of zeolite adsorption followed by counter-current desorption and catalytic combustion.

The zeolite beds and catalyst containers are designed as vertical cylinders, as presented in Figure 3 below. The pipes into the containers are widened with an angle α. To avoid pressure drops that may result in horizontal concentration gradients, α should be kept at no more than 20 degrees. It is only the cylindrical mid section that contains packing in the form of either zeolites or catalysts.

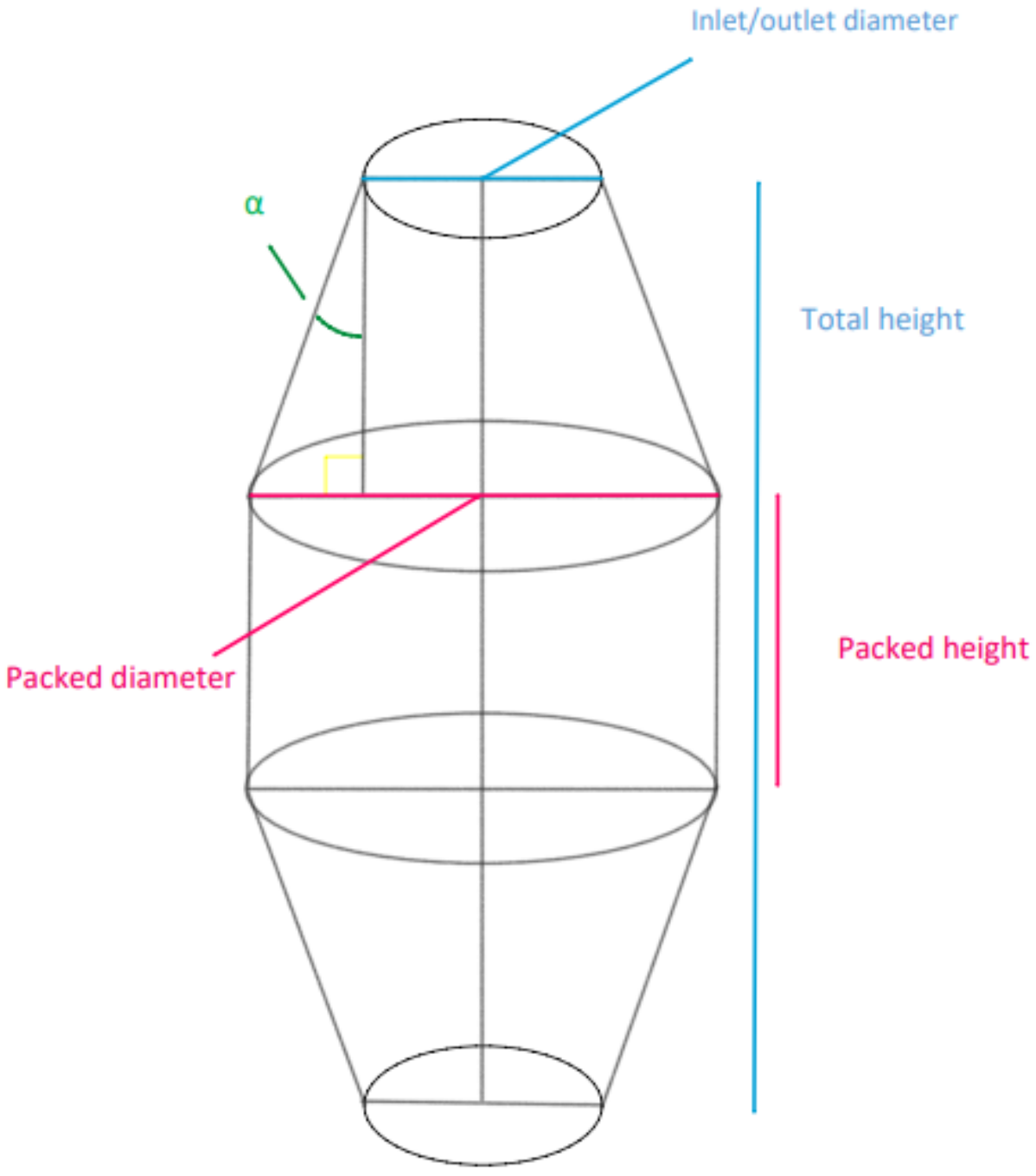

Figure 3: Vessel design of the zeolite beds and catalyst chamber.

5. Modelling and Assumptions

In chapter 5, models and assumptions that lay the foundation for the calculations presented in Appendix is discussed.

5.1. VOCs

The VOCs modelled were toluene, acetone, MEK, n-heptane and n-octane. Due to difficulties finding reliable data, all modelling was based on the VOC laden stream containing only one VOC at a time.

5.2. Adsorption

Modelling of the adsorption and breakthrough times was based on the Langmuir model in Hans Karlsson's *Adsorptionsanläggningar* (1977).

Due to difficulties finding relevant Langmuir constants, only toluene was modelled for a FAU Y zeolite (Andriantsiferana et al., 2015). The rest were modelled for a MFI silicalite zeolite (Brosillon et al., 2001).

Adsorption was assumed to occur instantly, and no concentration profile over the bed was regarded.

The mass transport phenomena modelled are axial dispersion, outer mass transport and pore diffusion.

The parameter $\frac{D_c}{a_c^2}$ in the expression of the pore diffusion was estimated but had little to no effect on the overall adsorption.

The calculations are presented in Appendix A.3.

5.3. Desorption and Regeneration

Modelling of the desorption and regeneration was based upon Hans Karlsson's *Adsorptionsanläggningar* (1977).

The time of regeneration is divided into three parts; the time to heat the zeolite bed, the time to heat the vessel containing the zeolites, and the time of desorption. Since the time it takes to heat up the zeolite bed to desorption temperature is much greater than both the two other terms, it is assumed that desorption starts taking place at the final 50 % of the total regeneration time. It is further assumed that desorption occurs at a constant rate.

The enthalpy of adsorption ΔH_{ads} was estimated with the total amount of moles adsorbed onto the bed n_{VOC} with the negative enthalpy of vaporization $-\Delta H_{vap}$.

The specific enthalpy of the regeneration medium H_f is calculated at the higher regeneration temperature T_2 to avoid under dimensioning of the regeneration time t_s.

The temperature of desorption was assumed to be sufficient at 200 °C (Yamauchi et al., 2007).

The calculations are presented in Appendix A.4.

5.4. Combustion

Modelling of the catalytic combustion was based upon the equivalence ratio Φ and the adiabatic flame temperature, and it is assumed that the rise in temperature during combustion is directly proportional to Φ. The adiabatic flame temperature of MEK was not found but estimated at 2300 K which is within the typical range of hydrocarbons combusted in air (2200-2500K). The temperature of combustion was assumed to be sufficient at 350 °C (Kima and Shim, 2010).

The calculations are presented in Appendix A.5.

5.5. Heat and Area Requirements

Again it was assumed that desorption starts taking place at the final 50 % of the total regeneration time. The heat released upon combustion is sufficient to reach the desorption temperature of 200°C. Thus, heat is required to Heat Coil 2 only for the first 50 % of the regeneration time.

Since VOCs are assumed to desorb only after 50 % of the regeneration time, heat to Heat Coil 1 is only required for the last 50 % of the regeneration time.

Differences in heat capacities, densities, and volumetric flows of the air due to varying VOC concentrations and temperatures are considered minor and are neglected. Since the system is considered to be in steady-state, it follows that all streams are of equal mass flows. It further follows that 1 °C increase in the regeneration stream equals 1 °C decrease in the heat source stream.

The typical max efficiency of a heat exchanger is 70 % of total available heat. Since less than 70 % of total available heat after combustion is sufficient to reach desorption temperatures, this is not an issue that needs to be considered.

The calculations are presented in Appendix A.6.

5.6. Costs

Capital costs are estimated using the software tool EconExpert developed by P.T. Vasudevan and T. Ulrich. During estimates of the zeolite beds and the catalyst, this includes the purchases of the first batches zeolites and actual catalyst, which later become operational costs. Note that the investment would be brownfield (existing facilities) rather than greenfield (new facilities); thus auxiliary facility costs are neglected, and the cost of interest is presented as *Total module cost* in Section 6.5.1.

The life expectancy of the facility is 25 years, and the interest rate is estimated at 5 %. Maintenance and repair costs are estimated at 6 % of total grass roots capital, and spare part costs at 15 % of maintenance and repair costs.

The calculations are presented in appendix A.7.

6. Results

In Chapter 6, the most relevant results of the calculations in Appendix are presented. This includes general dimensions of vessels, zeolite and catalyst masses, breakthrough and regeneration times of the zeolites, temperatures upon combustion and heat requirements, as well as capital and operational costs.

6.1. Dimensions

In section 6.1., some general dimensions of the zeolite and catalyst vessels are presented. If uncertain about what is being presented, the reader is referred to Figure 3 in Section 4.3.

Table 6: Dimensions of the zeolite beds (per bed).

Wall thickness [mm]	2
Enlargement angle α [degrees]	20
Packed height [m]	1
Total height [m]	5.07
Packed section diameter [m]	1.96
Inlet/outlet diameter [m]	0.48
Inlet/outlet velocity [m/s]	10
Zeolite [kg]	1393
Stainless steel [kg]	249.1

Table 7: Dimensions of the catalyst bed.

Wall thickness [mm]	2
Enlargement angle α [degrees]	20
Packed height [m]	1.11
Total height [m]	2.54
Packed section diameter [m]	1
Inlet/outlet diameter [m]	0.48
Inlet/outlet velocity [m/s]	10
Catalyst [kg]	610
Stainless steel [kg]	85.6

6.2. Volumetric Flows, Concentrations, and Breakthrough and Regeneration Times

In section 6.2., the main results of interest are the breakthrough and regeneration times of the zeolite beds. The results regard each bed individually, and so after a breakthrough has occurred, the VOC laden air stream may be switched to the empty bed as the full bed is regenerated.

For multiple answers, the VOCs are listed in order:

Toluene – Acetone - MEK - n-Heptane - n-Octane

Table 8: Resulting breakthrough and regeneration times of the zeolite beds (per bed), with some complementary data.

Volumetric flow during adsorption [m^3/s]	1.82
VOC concentration into adsorber [g/m^3]	0.09
Breakthrough times [h]	[65.7 35.1 50.7 31.0 24.5]
Volumetric flow during regeneration [m^3/s]	1.82
Temperature during regenerationdd [°C]	200
VOC concentrations during desorption [g/m^3]	[86.2 49.0 67.5 44.6 36.0]
Regeneration times [h]	[0.11 0.11 0.11 0.11 0.10]
Rate of temperature increase in zeolite bed during regeneration [°C/min]	33.6

6.3. Heat Exchangers and Heating Coils

In this section, heat requirements and heating equipment are presented. Due to modelling and the assumptions made, the areas of the various units become the same. The derivation of this is presented in Appendix A.6.

For multiple answers, the VOCs are listed in order:

Toluene – Acetone - MEK - n-Heptane - n-Octane

Table 9: Heat and heating area requirements.

Area (per unit) [m^2]	87.7
Heat requirement Heat Coil 1 (20 to 200 °C) [kW]	393.5
Heat requirement Heat Coil 1 [kWh/year]	[3064 5367 3881 5912 7328]
Heat requirement Heat Coil 2 (200 to 350 °C) [kW]	327.9
Heat requirement Heat Coil 2 [kWh/year]	[2554 4472 3234 4927 6106]
Total heat requirement [kWh/year]	**[5618 9839 7115 10 839 13 434]**

6.4. Catalytic Combustion

The equivalence ratio Φ and resulting temperatures upon combustion are presented below.

For multiple answers, the VOCs are listed in order:

Toluene – Acetone - MEK - n-Heptane - n-Octane

Table 10: Equivalence ratio Φ and resulting temperatures upon combustion.

Temperature into catalyst [°C]	350
Equivalence ratio Φ	[0.20 0.08 0.12 0.12 0.09]
Temperature after catalytic combustion [°C]	[759 511 601 608 541]

6.5. Costs

Capital and operational costs are here presented, as well as annuity and depreciation costs. Note

6.5.1. Capital Costs

Capital costs are estimated with the Chemical engineering plant cost index (CEPCI) of 2020 (596.2).

The price of the zeolites is estimated at 20 $/kg.

The price of the catalyst is estimated at 50 $/kg.

Note that the investment would be *brownfield*, and the cost of interest is presented as *Total module cost*.

Table 11: Capital costs.

Unit	**Bare module cost per unit [SEK] (1 $ = 10.00 SEK)**	**Number of units**
Zeolite beds (including zeolites)	3,903,440	2
Catalyst bed (including catalyst)	1,802,380	1
Heat exchanger	415,580	1
Heating coils	415,580	2
Fans	122,810	3
Total bare module cost [SEK]	10,856,000	
Contingency and fee [SEK]	1,954,080	
Total module cost [SEK]	12,810,080	
Auxiliary facilities [SEK]	3,973,450	
Grass roots capital [SEK]	17,218,300	

Annuity and depreciation are presented at the estimated life expectancy and interest rate below.

Table 12: Annuity and depreciation costs.

Life expectancy [Years]	25
Interest rate [%]	5
Maintenance and repair annuity costs [SEK/year]	73,300
Spare parts annuity costs [SEK/year]	10,100
Depreciation [SEK/year]	512,400
Total annuity and depreciation [SEK/year]	595,800

6.5.2. Operational Costs

Operational costs regarded are heat requirements, zeolites and catalyst.

It is assumed that the zeolite will last for 10 years and the catalyst for 2 years.

The price of the zeolites is estimated at 20 $/kg = 200 SEK/kg.

The price of the catalyst is estimated at 50 $/kg = 500 SEK/kg.

The price of electricity is estimated at 1.5 SEK/kWh.

Total yearly usage of electricity is estimated at 20,000 kWh/year.

Table 13: Operational costs accounting for catalyst and zeolite life expectancies.

Year	**Yearly cost [SEK/year]**
0-2	30,000
2-10	182,500
10+	238,220

6.5.3. Total Yearly Costs

One final table is produced for better overview of the total yearly costs. Costs for total annuity and depreciation and operational costs are summarized and presented in Table 14 below.

Table 14: Total yearly costs.

Year	**Total yearly cost [SEK/year]**
0-2	625,800
2-10	778,300
10+	834,020

7. Discussion

The relatively few VOCs of interest in this report have been made plausible through a brief investigation of common volatile hydrocarbons used in larger industries that are customers of Sysav, especially at the wastewater treatment plant at the department for hazardous waste. If the actual VOCs present differs much from those assumed, several issues could, of course, arise. One plausible issue is that the VOC laden streams may contain hydrocarbons of greater sizes than is accounted for in this report. If these molecules are sufficiently large, the molecules will become entrapped within the pores and clog up the pore channels, effectively deteriorating the zeolites over time.

If certain VOCs coexist and simultaneously are concentrated during adsorption and desorption, unpredicted reactions may occur. Spontaneous reactions between hydrocarbons are almost exclusively exothermic. Thus there is a risk of sudden random heat spots arising. This is typically combatted by continuously monitoring temperatures in various places throughout the column but is not as crucial for zeolites as for a flammable carbon bed.

Another issue when dealing with a mixture of VOCs is the competition of the active sites of the catalyst. When different VOCs compete for the active sites, higher temperatures are required to speed up the combustion and make a place at the site for the next molecule. This, in turn, of course, increases operational costs due to increased required heating.

The low heat requirements presented in Section 5.5 are probably highly misleading and underestimated. These are the results of the simplified steady-state modelling and the single component assumption. The issue of the heating rate of the zeolites is also neglected: as a rule of thumb, this should not exceed 1 °C per minute, as tensions within the zeolite materials may cause them to crack and break. As for now, this rate is much too high, thus allowing a much faster regeneration and lower heat requirements.

Further treatment steps could be implemented in the suggested process. One possible implementation could be a selective ammonia catalyst before the Mn_3O_4 main catalyst to prevent the formation of NO_x species as well as possible deposition of formed ammonium chloride when the exhaust gas cools down. Another possible implementation could be a water-based scrubber to treat hydrochloric acid and other water-soluble species. Whether this should be implemented before or after the Mn_3O_4 catalyst would have to be determined based on the qualities and quantities of the present VOCs and their possible products when combusted in the presence of the acid. A third implementation could be an alkaline adsorbent to adsorb chlorine before combustion to prevent the formation of chlorinated species, such as the ammonium chloride mentioned above.

8. Future Work

The most important possible future work is to determine both qualitatively and quantitatively what VOCs are present. This would allow for better suggestions and more accurate predictions. Qualitatively, this would have to be done with air samples from the water treatment plant on multiple occasions and for a wider variety of VOCs than investigated in this study. Quantitatively, a continuous FID could be implemented over a longer timespan to monitor possible variations in concentrations, as these may vary during nighttime or weekends.

If the VOCs were better known, more advanced modelling of the problems would give better predictions of the outcome. This would include time-dependent models of differential equations and not just simplified equations for a steady-state system as-is for now.

If modelling of the problem could be carried out more accurately, further optimization would be of great importance. A more conscious design of the columns and vessels could possibly decrease capital costs greatly. Optimization would also include a more thorough investigation of the best suitable zeolites and catalyst, and possible better heat recovery.

Finally, if a zeolite-catalyst solution was to be employed, a pilot-scale on-site test facility would be a necessary first step. This would give more definite indications than any modelling ever could.

9. References (Alphabetically by Title)

A. O'Reilly (1998), *A Series Reaction Approach to VOC Incineration*, Process Safety and Environmental Protection, Volume 76, Issue 4, Pages 302-312, ISSN 0957-5820, https://doi.org/10.1205/095758298529669

Hans Karlsson (1977), *Adsorptionsanläggningar*, Tekniska Högskolan I Lund, Kemicentrum, Avdelning för Kemisk teknologi

W. John Thomas & Barry Crittenden (1998), *Adsorption Technology & Design*, 1st Edition, eBook ISBN: 9780080489971 (Thomas and Crittenden,1998)

Shengnan Song, Siyuan Zhang, Xiaolong Zhang, Priyanka Verma and Meicheng Wen (2020), *Advances in Catalytic Oxidation of Volatile Organic Compounds over Pd-Supported Catalysts: Recent Trends and Challenges*, Frontiers in Materials vol. 7, DOI: 10.3389/fmats.2020.595667, ISSN: 2296-8016 (Wen et al.)

H. Saito (2004), *Assessment of Industrial VOC Gas-Scrubber Performance*, US Department of Energy (US), Lawrence Livermore National Lab. (LLNL), Livermore, CA (United States)

Ch. Baerlocher, L.B. McCusker and D.H. Olson (2007), *Atlas of Zeolite Framework Types*, 6th edn., Elsevier, London

William M. Moe & Bing Qi (2005), *Biofilter Treatment of Volatile Organic Compound Emissions from Reformulated Paint: Complex Mixtures*, Intermittent Operation, and Startup, Journal of the Air & Waste Management Association, 55:7, 950-960, DOI: 10.1080/10473289.2005.10464687

Sang Chai Kima and Wang Geun Shim (2010), *Catalytic combustion of VOCs over a series of manganese oxide catalysts*, Applied Catalysis B: Environmental, Volume 98, Issues 3–4, Pages 180-185, DOI: https://doi.org/10.1016/j.apcatb.2010.05.027 (Kima and Shim, 2010)

F.N. Aguero, Bibiana P. Barbero, Luis Gambaro, Luis E. Cadus (2009), *Catalytic combustion of volatile organic compounds in binary mixtures over MnOx/Al2O3 catalyst*, Applied Catalysis B: Environmental, Volume 91, Pages 108–112, DOI: 10.1016/J.APCATB.2009.05.012 (Aguero et al., 2009)

Junlin Zeng, Xiaolong Liu, Jian Wanga, Hanlei Lv and Tingyu Zhu (2015), *Catalytic oxidation of benzene over MnOx/TiO2 catalysts and the mechanism study*, Journal of Molecular Catalysis A: Chemical, Volume 408, Pages 221-227, DOI: https://doi.org/10.1016/j.molcata.2015.07.024 (Zhu et al., 2015)

L.F. Liotta (2010), *Catalytic oxidation of volatile organic compounds on supported noble metals*, Applied Catalysis B: Environmental, Volume 100, Issues 3–4, Pages 403-412, DOI: https://doi.org/10.1016/j.apcatb.2010.08.023 (Liotta, 2010)

Nunez*, C, G. Ramsey*, L. Hamel, AND P. Kariher (1993), *CORONA DESTRUCTION: AN INNOVATIVE CONTROL TECHNOLOGY FOR VOCS AND AIR TOXICS*, JOURNAL OF

AIR AND WASTE MANAGEMENT, Air & Waste Management Association, Pittsburgh, PA, 43(2):242-247

Structure Commission of the International Zeolite Association (IZA-SC), *Database of Zeolite Structures*, website: https://europe.iza-structure.org/IZA-SC/ftc_table.php, Last visited: 9 December 2021, Copyright: 2017

Michael Kosusko & Carlos M. Nunez (1990), *Destruction of Volatile Organic Compounds Using Catalytic Oxidation*, Journal of the Air & Waste Management Association, 40:2, 254-259, DOI: 10.1080/10473289.1990.10466682

Emmerich Wilhelm and Rubin Battino (1971), *Estimation of Lennard-Jones (6,12) Pair Potential Parameters from Gas Solubility Data*, J. Chem. Phys. vol. 55, https://doi.org/10.1063/1.1676694

Brodu, Nicolas and Sochard, Sabine and Andriantsiferana, Caroline and Pic, Jean-Stéphane and Manero, Marie-Hélène (2015), *Fixed-bed adsorption of toluene on high silica zeolites: experiments and mathematical modelling using LDF approximation and a multisite model*. Environmental Technology, 36 (14). 1807-1818. ISSN 0959-3330
(Andriantsiferana et al., 2015)

Philip L. Llewellyn and Guillaume Maurin (2007), *Gas Adsorption In Zeolites and Related Materials*, Introduction To Zeolite Science and Practice, Studies in Surface Science and Catalysis Vol. 168, 3rd Revised Edition, ISBN: 978-0-444-53063-9

Hisashi Yamauchi, Akio Kodama, Tsutomu Hirose, Hiroshi Okano, and Ken-ichiro Yamada (2007), *Industrial & Engineering Chemistry Research* **2007** *46* (12), 4316-4322, DOI: 10.1021/ie061184e

Jiří Čejka, Herman van Bekkum, Avelino Corma, and Ferdi Schüth (editors) (2007), *Introduction To Zeolite Science and Practice*, Studies in Surface Science and Catalysis Vol. 168, 3rd Revised Edition, ISBN: 978-0-444-53063-9

Stephan Brosillon, Marie-Helene Manero, and Jean-Noel Foussard (2001), *Mass Transfer in VOC Adsorption on Zeolite: Experimental and Theoretical Breakthrough Curves*, Environ. Sci. Technol. 2001, 35, 17, 3571–3575, https://doi.org/10.1021/es010017x

Hisashi Yamauchi, Akio Kodama, Tsutomu Hirose, Hiroshi Okano, and Ken-ichiro Yamada (2007), *Performance of VOC Abatement by Thermal Swing Honeycomb Rotor Adsorbers*, Industrial & Engineering Chemistry Research 2007 46 (12), 4316-4322, DOI: 10.1021/ie061184e (Yamauchi et al., 2007)

Birte Mull, Lennart Möhlmann and Olaf Wilke (2017), *Photocatalytic Degradation of Toluene, Butyl Acetate and Limonene under UV and Visible Light with Titanium Dioxide-Graphene Oxide as Photocatalyst*, Bundesanstalt für Materialforschung und-prüfung (BAM)

Chihara, K., Smith, J.M. and Suzuki, M. (1981), *Regeneration of powdered activated carbon. Part I. Thermal decomposition kinetics*, AIChE J., 27: 213-220. https://doi.org/10.1002/aic.690270207

Huang Y, Ho SS, Lu Y, Niu R, Xu L, Cao J, Lee S., *Removal of Indoor Volatile Organic Compounds via Photocatalytic Oxidation: A Short Review and Prospect*, Molecules. 2016 Jan 4;21(1):56. doi: 10.3390/molecules21010056. PMID: 26742024; PMCID: PMC6273848.

Zhishu Liang, Jijun Wang, Yuna Zhang, Cheng Han, Shengtao Ma, Jiangyao Chen, Guiying Li and Taicheng An, *Removal of volatile organic compounds (VOCs) emitted from a textile dyeing wastewater treatment plant and the attenuation of respiratory health risks using a pilot-scale biofilter*, Journal of Cleaner Production, Volume 253, 2020, 120019, ISSN 0959-6526, https://doi.org/10.1016/j.jclepro.2020.120019. (https://www.sciencedirect.com/science/article/pii/S0959652620300664)

D.H. Kim, M.C. Kung, A. Kozlova, S.D. Yuan and H.H. Kung (2004), *Synergism between Pt/Al2O3 and Au/TiO2 in the low temperature oxidation of propene*, Catalysis Letters Vol. 98, DOI: 10.1007/s10562-004-6440-z (Kozlova et al., 2004)

Ki-Joong Kim and Ho-Geun Ahn (2011), *The effect of pore structure of zeolite on the adsorption of VOCs and their desorption properties by microwave heating*, Microporous and Mesoporous Materials, Volume 152, 1 April 2012, Pages 78-83, https://doi.org/10.1016/j.micromeso.2011.11.05

H. von Kienle, N. Kunze, D.H. Mertens (1994), *The Use of Activated Carbon in the Removal of VOC's*, Studies in Environmental Science, Elsevier, Volume 61, Pages 321-329, ISSN: 0166-1116, ISBN: 9780444817891

Theo Maesen (2007), *The Zeolite Scene – An Overview*, Introduction To Zeolite Science and Practice, Studies in Surface Science and Catalysis Vol. 168, 3rd Revised Edition, ISBN: 978-0-444-53063-9

Liyan Qiu (2000), *Thermal Properties of Framework Materials: Selected Zeoiites, Clathrates and an Organic Diol*, Dalhousie University Halifax, Nova Scotia, Pages 86-87

Clean Air Technology Center (CATC) (1998), *Zeolite – A versatile air pollutant adsorber*, Information Transfer and Program Integration Division Office of Air Quality Planning and Standards U.S. Environmental Protection Agency

Lynne B. McCusker and Christian Baerlocher (2007), *Zeolite Structures*, Introduction To Zeolite Science and Practice, Studies in Surface Science and Catalysis Vol. 168, 3rd Revised Edition, ISBN: 978-0-444-53063-9

Appendix

A.0. Denotation Index

$A = Area\ [m^2]$

$A_T = Area\ of\ heat\ exchanger\ or\ heating\ coil\ [m^2]$

$a_p = The\ specific\ outer\ area\ of\ the\ adsorbent\ [m^2/m^3]$

$b = Thickness\ of\ cylindrical\ adsorbed\ wall\ [m]$

$C_{pads} = Specific\ heat\ capacity\ of\ the\ adsorbate\ [J/(kg \cdot K)]$

$C_{pf} = Specific\ heat\ capacity\ of\ the\ fluid\ (air)\ [J/(kg \cdot K)]$

$C_{ps} = Specific\ heat\ capacity\ of\ the\ adsorbent\ [J/(kg \cdot K)]$

$C_{pst} = Specific\ heat\ capacity\ of\ the\ adsorber\ [J/(kg \cdot K)]$

$c = Any\ given\ concentration\ [mol/m^3]$

$c_{reg} = Concentration\ upon\ desorption\ [mol/m^3]$

$c_0 = Inlet\ concentration\ [mol/m^3]$

$c_{0,mg} = Inlet\ concentration\ [mg/m^3]$

$c_2 = Outlet\ concentration\ [mol/m^3]$

$D = Adsorber\ diameter\ [m]$

$D_c = Intercrystalline\ diffusion\ constant\ [m^2/s]$

$D_f = Molecular\ diffusion\ constant\ [m^2/s]$

$D_p = Solid\ phase\ diffusion\ constant\ [m^2/s]$

$D_{pore} = Pore\ diffusion\ constant\ [m^2/s]$

$d_p = Particle\ diameter\ [m]$

$f_A = Annuity\ factor$

$f_{ht} = Correction\ factor$

$f_{MnR} = Maintenance\ and\ repair\ factor$

$f_{sep} = Separation\ factor$

$f_{Spare} = Spare\ parts\ factor$

$G_{sep,pore} = Separation\ variable\ for\ pore\ diffusion$

$G_{sep,p} = Separation\ variable\ for\ solid\ phase\ diffusion$

$H_f = Specific\ enthalpy\ of\ the\ regeneration\ medium\ [J/kg]$

$\Delta H_{ads} = Enthalpy\ of\ adsorption\ [J]$

$\Delta H_{vap} = Enthalpy\ of\ vaporization\ [J/mol]$

$h_1 = Heat\ transfer\ rate, cold\ side\ [W/(m^2 \cdot K)]$

$h_2 = Heat\ transfer\ rate, hot\ side\ [W/(m^2 \cdot K)]$

$h_f = Heat\ transfer\ coefficient\ of\ the\ medium\ (air)\ [W/(m^2 \cdot K)]$

$h_s = Heat\ transfer\ coefficient\ of\ the\ adsorbent\ [W/(m^2 \cdot K)]$

$h_t = Total\ heat\ transfer\ coefficient\ of\ the\ medium\ and\ adsorbent\ [W/(m^2 \cdot K)]$

$j_h = Correlation\ factor\ of\ the\ heat\ transfer$

$K = Langmuir\ equilibrium\ constant\ [m^3/(mol \cdot Pa)]$

$k = Fictive\ mass\ transfer\ coefficient\ [s^{-1}]$

$k_d = k\ for\ the\ dispersion\ [s^{-1}]$

$k_e = k\ for\ the\ full\ system\ [s^{-1}]$

$k_f = k\ for\ the\ media\ film\ [s^{-1}]$

$k_p = k\ for\ the\ solid\ phase\ [s^{-1}]$

$k_{por} = k\ for\ the\ pores\ [s^{-1}]$

$L = Equivalent\ length\ of\ dispersion\ [m]$

$L_T = Wall\ thickness\ of\ heat\ exchanger\ [m]$

$M_A = The\ "molecular\ weight"\ of\ air\ [g/mol]$

$MnR_{Annual} = Annual\ costs\ of\ maintenance\ and\ repair\ [SEK/year]$

$M_{N2} = Molecular\ weight\ of\ nitrogen\ [g/mol]$

$M_{O2} = \ Molecular\ weight\ of\ oxygen\ [g/mol]$

$M_w \ = \ Molecular\ weight\ [g/mol]$

$m = Mass\ [kg]$

$m_g = Mass\ [g]$

$m_{st} = Jacket\ mass\ of\ cylindrical\ adsorber\ [kg]$

$m_{VOC} = Total\ amount\ of\ VOCs\ adsorbed\ onto\ bed\ [kg]$

$m_{vol} = Jacket\ volume\ of\ cylindrical\ adsorber\ [m^3]$

$m_Z = Zeolite\ mass\ [kg]$

$N = Number\ of\ transfer\ units$

$N_A \ = \ Avogadro\ constant\ [mol^{-1}]$

$N_d = N\ for\ the\ dispersion$

$N_f = N\ for\ the\ film$

$N_{por} = N\ for\ the\ pore\ diffusion$

$N_Y = Life\ expectancy\ [years]$

$n = Amount\ [mol]$

$n_{Air,\Phi=1,tot}$
$= Total\ number\ of\ "air\ molecules"\ during\ desoprtion\ at\ stoichiometric\ combustion\ [mol]$

$n_{Air,des,tot} = Total\ number\ of\ "air\ molecules"\ during\ desoprtion\ [mol]$

$n_C = Number\ of\ carbon\ atoms\ present\ in\ the\ VOC\ specimen$

$n_H = Number\ of\ hydrogen\ atoms\ present\ in\ the\ VOC\ specimen$

$n_O = Number\ of\ oxygen\ atoms\ present\ in\ the\ VOC\ specimen$

$n_{O2,\Phi=1}$
$= Number\ of\ oxygen\ molecules\ requirred\ per\ stoichiometric\ combustion\ reaction$
$[molecules/reaction]$

$n_{O2,\Phi=1,tot}$
$= Total\ number\ of\ oxygen\ molecules\ requirred\ for\ combustion\ of\ all\ VOC\ [mol]$

$n_{VOC} = Total\ amount\ of\ VOCs\ adsorbed\ onto\ bed\ [mol]$

$Pe = Peclets\ number$

$Q = Heat\ supplied\ to\ the\ system\ [W]$

$\dot{Q}_{ads} = Volumetric\ flow\ of\ adsorption\ medium\ [m^3/s]$

$\dot{Q}_{reg} = Volumetric\ flow\ of\ regeneration\ medium\ [m^3/s]$

$q = Adsorbed\ amount\ at\ any\ given\ concentration\ c\ [mol/kg]$

$q_0 = Adsorbed\ amount\ at\ equilibrium\ \ at\ concentration\ c_0\ [mol/kg]$

$q_2 = Adsorbed\ amount\ at\ equilibrium\ \ at\ concentration\ c_2\ [mol/kg]$

$q_{max} = Maximum\ adsorption\ capacity\ [mol/kg]$

$R = Gas\ constant\ [J/(mol \cdot K)]$

$R' = Langmuirs\ separation\ factor$

$Re = Reynolds\ number$

$r_p\ = \ Spherical\ molecular\ radius\ [m/molecule]$

$Sc = Schmidts\ number$

$Spare_{Annual} = Annual\ costs\ of\ spare\ parts\ [SEK/year]$

$T_1 = Initial\ temperature\ of\ the\ regeneration\ [K]$

$T_2 = Final\ temperature\ of\ the\ regeneration\ [K]$

$T_{ad} = Adiabatic\ flame\ temperature\ at\ stoichiometric\ combustion\ in\ air\ [K]$

$T_{ad,cat} = Temperature\ after\ catalytic\ combustion\ [K]$

$T_{ad,rise} = Rise\ in\ temperature\ upon\ catalytic\ combustion\ [K]$

$T_{in,cat} = Temperature\ in\ to\ catalyst\ [K]$

$T_{out,cat} = Temperature\ after\ catalytic\ combustion\ and\ heat\ exchange\ [K]$

$\Delta T = Temperature\ rise\ of\ the\ regeneration\ [K]$

$\Delta T_L = Logarithmic\ mean\ temperature\ [K]$

$\Delta T_{L,1} = First\ term\ of\ the\ logarithmic\ mean\ temperature\ [K]$

$\Delta T_{L,2} = Second\ term\ of\ the\ logarithmic\ mean\ temperature\ [K]$

$T_s' = Correction\ factor\ (> 1)$

$T' = Transfer\ parameter$

$T_d = T'\ for\ the\ dispersion$

$T_f = T'\ for\ the\ outer\ mass\ transport$

$T_{por} = T'\ for\ the\ pore\ diffusion$

$T_p = T'\ for\ the\ solid\ phase$

$t_{1/2} = Ideal\ breakthrough\ time\ (upper\ limit)\ [s]$

$\hat{t} = Breakthrough\ time\ [s]$

$t_{des} = Desorption\ time\ [s]$

$t_s = Regeneration\ time\ [s]$

$U = Overall\ heat\ transfer\ coefficient\ [W/(m^2 \cdot K)]$

$V = Volume\ [m^3]$

$V_{ads} = Actual\ velocity\ of\ adsorption\ medium\ through\ bed\ [m/s]$

$V_{0,ads} = Velocity\ of\ adsorption\ medium\ through\ empty\ bed\ [m/s]$

$V_{reg} = Actual\ velocity\ of\ regeneration\ medium\ through\ bed\ [m/s]$

$V_{0,reg} = Velocity\ of\ regeneration\ medium\ through\ empty\ bed\ [m/s]$

$V_m\ =\ Spherical\ molecular\ volume\ [m^3/molecule]$

$x_2 = Adsorber\ height\ [m]$

$x_{moist} = Humidity$

$x_{int} = Interest\ rate$

$X = Outlet\ concentration\ divided\ by\ inlet\ concentration\ at\ breakthrough\ time$

Y
$= Adsorbed\ amount\ at\ outlet\ divided\ by\ adsorbed\ amount\ at\ inled\ at\ breakthrough\ time$

$\delta = Separation\ factor$

$\delta_d = \delta\ for\ the\ dispersion$

$\delta_f = \delta\ for\ the\ outer\ mass\ transport$

$\delta_p = \delta\ for\ the\ pore\ diffusion$

$\epsilon = Void$

$\theta_{ads} = Adsorption\ medium\ residence\ time\ [s]$

$\theta_{reg} = Regeneration\ medium\ residence\ time\ [s]$

$\varkappa = Heat\ conductivity\ of\ the\ regeneration\ medium\ [J/(m \cdot K \cdot s)]$

$\lambda_T = Thermal\ conductivity\ [W/(m \cdot K)]$

$\mu = The\ dynamic\ viscosity\ [kg/(m \cdot s)]$

$\xi = Form\ factor$

$\rho_A = Air\ density\ (regeneration\ medium)\ [kg/m^3]$

$\rho_B = Zeolite\ bulk\ density\ [kg/m^3]$

$\rho_L = Liquid\ mass\ density\ at\ room\ temperature\ [kg/m^3]$

$\rho_{molar} = Liquid\ molar\ density\ at\ room\ temperature\ [moles/m^3]$

$\rho_S = Stainless\ steel\ density\ [kg/m^3]$

$\upsilon = The\ kinematic\ viscosity\ [m^2/s]$

$\psi_p = Correction\ factor\ for\ the\ concentration\ profile\ in\ the\ solid\ phase\ [-]$

$\psi_{por} = Correction\ factor\ for\ the\ concentration\ profile\ in\ the\ pores\ [-]$

A.1. General Expressions

$$V = \frac{V_0}{\epsilon}\ [m/s]$$

$$A = \frac{\dot{Q}}{V_0} = \frac{\dot{Q}}{V \cdot \varepsilon}\ [m^2]$$

$$D = \sqrt{\frac{4 \cdot A}{\pi}}\ [m]$$

$$m_Z = \rho_B \cdot A \cdot x_2\ [kg]$$

$$\theta = \frac{x_2}{V}\ [s]$$

$$t_{1/2} = \frac{\rho_B \cdot q_0 \cdot \theta}{c_0 \cdot \epsilon} + \theta\ [s]$$

$$\hat{t} = \frac{\rho_B \cdot q_0 \cdot \theta}{c_0 \cdot \epsilon} \cdot T' + \theta\ [s]$$

$$T' = min\left[T_d, T_f T_r, max\left[T_{por}, T_p\right]\right]$$

$$T' = f\left(N, X, f_{sep}, \delta\right)$$

$$N = k_e \cdot a_p \cdot \frac{\theta}{\epsilon}$$

$$k_e \cdot a_p = \frac{\epsilon \cdot x_2}{\theta \cdot L}\ [s^{-1}]$$

$$N = \frac{x_2}{L}$$

$$f_{sep} = R' = \frac{X \cdot (1 - Y)}{Y \cdot (1 - X)}$$

$$q = q_{max} \cdot \frac{K \cdot c}{1 + K \cdot c}\ [mole/kg]$$

$$X = \frac{c_2}{c_0}$$

$$Y = \frac{q_2}{q_0}$$

$$a_p \approx \frac{6 \cdot (1 - \epsilon)}{d_p}\ [m^2/m^3]$$

$$\lambda = \frac{q_0 \cdot \rho_B}{c_0}$$

$$M_w = \frac{m_g}{N}\ [g/mol]$$

$$\rho = \frac{m}{V}\ [kg/m^3]$$

$$\rho_{molar} = \frac{\rho}{M_w \cdot 10^{-3}}\ [mol/m^3]$$

$$V_m = \frac{1}{\rho_{molar} \cdot N_A}\ [m^3/molecule]$$

$$P \cdot V = n \cdot R \cdot T\ [J]$$

A.2. Spherical Molecular Diameter

$$V_m = \frac{4}{3} \cdot \pi \cdot r_p^3 \ [m^3] \rightarrow d_p = 2 \cdot \sqrt[3]{\frac{3}{4} \cdot \frac{1}{\pi} \cdot V_m} \ [m]$$

A.3. Langmuir Adsorption and Breakthrough Times for Zeolites

For multiple answers, the VOCs are listed in order:

Toluene – Acetone - MEK - n-Heptane - n-Octane

A.3.1. Set/Calculated General Dimensions and Variables with Constants Found in Literature

$\dot{Q}_{ads} = 1.8164\ [m^3/s]$

$\epsilon = 0.40$

$V_{0,ads} = 0.60\ [m/s]$

$$V_{ads} = \frac{V_{0,ads}}{\epsilon}$$

$$A = \frac{\dot{Q}_{ads}}{V_{0,ads}} = \frac{\dot{Q}_{ads}}{V_{ads} \cdot \epsilon}$$

$$D = \sqrt{\frac{4 \cdot A}{\pi}}$$

$x_2 = 1.0\ [m]$

$\rho_B = 460\ [kg/m^3]$

$m_Z = \rho_B \cdot A \cdot x_2$

$$\theta_{ads} = \frac{x_2}{V_{ads}}$$

$M_w = [92.14\ \ 58.08\ \ 72.11\ \ 100.21\ \ 114.23]\ [g/mol]$

$c_{0,mg} = 90\ [mg/m^3]$

$c_0 = [0.0010 \quad 0.0015 \quad 0.0012 \quad 0.0009 \quad 0.0008]\ [mol/m^3]$

$c_2 = 0.10 \cdot c_0\ [mol/m^3]$

$$X = \frac{c_2}{c_0} = 0.10$$

$K = [1456\ 165\ 269\ 250\ 253]\ \left[[m^3/(mol \cdot Pa)]\right]$ (Brosillon et al., 2001, Andriantsiferana et al., 2015)

$q_{max} = [1.91\ 1.28\ 1.2\ 0.73\ 0.56]\ [mol/kg]$ (Brosillon et al., 2001, Andriantsiferana et al., 2015)

$q_0 = q_{max} \cdot \frac{K \cdot c_0}{1+K \cdot c_0} \, [mol/kg]$

$q_2 = q_{max} \cdot \frac{K \cdot c_2}{1+K \cdot c_2} \, [mol/kg]$

$Y = \frac{q_2}{q_0}$

$f_{sep} = R' = \frac{X \cdot (1-Y)}{Y \cdot (1-X)}$

$\upsilon = 1.48 \cdot 10^{-5} \, [m^2/s]$

$D_f = 1.11 \cdot 10^{-9} \, [m^2/s]$

$Sc = \frac{\upsilon}{D_f}$

$Pe = 2.0$, for gases in both the laminar and turbulent region.

$d_p = 4.1 \, [mm]$ (spherical pellets)

$Re = \frac{d_p \cdot V_{ads} \cdot \varepsilon}{\upsilon}$

$L = \frac{d_p}{Pe} + \frac{D_f \cdot \theta_{ads}}{2 \cdot \varepsilon \cdot x_2}$

$\delta_p, \delta_d, \delta_f$, table values found in Karlsson, 2010.

$\frac{D_c}{d_c^2} = 1.0 \cdot 10^{-4} \, [s^{-1}]$

$\lambda = \frac{q_0 \cdot \rho_B}{c_0}$

A.3.2. Dispersion

$$N_d = \frac{x_2}{L}$$

$$\frac{1}{1-R'} \cdot ln\frac{1}{1-X} + \frac{R'}{1-R'} \cdot lnX = N_d \cdot (T_d' - 1) + \delta_d \rightarrow$$

$$T_d' = \frac{\left[\frac{1}{1-R'} \cdot ln\frac{1}{1-X} + \frac{R'}{1-R'} \cdot lnX - \delta_d\right]}{N_d} + 1$$

A.3.3. Outer Mass Transport

$$k_e \cdot a_p = k_f \cdot a_p = 1.13 \cdot a_p \cdot V_{0,ads} \cdot (Re)^{-0.42} \cdot (Sc)^{-\frac{2}{3}}$$

$$N_f = k_e \cdot a_p \cdot \frac{\theta_{ads}}{\epsilon} = k_f \cdot a_p \cdot \frac{\theta_{ads}}{\epsilon}$$

$$\frac{1}{1-R'} \cdot lnX - \frac{R'}{1-R'} \cdot \ln(1-X) = N_f \cdot \left(T_f' - 1\right) + \delta_f \rightarrow$$

$$T_f' = \frac{\left[\frac{1}{1-R'} \cdot lnX - \frac{R'}{1-R'} \cdot \ln(1-X) - \delta_f\right]}{N_f} + 1$$

A.3.4. Pore Diffusion

$N_{pore} \cdot (T'_{pore} - 1) = -\{Length\}$, from extrapolation:

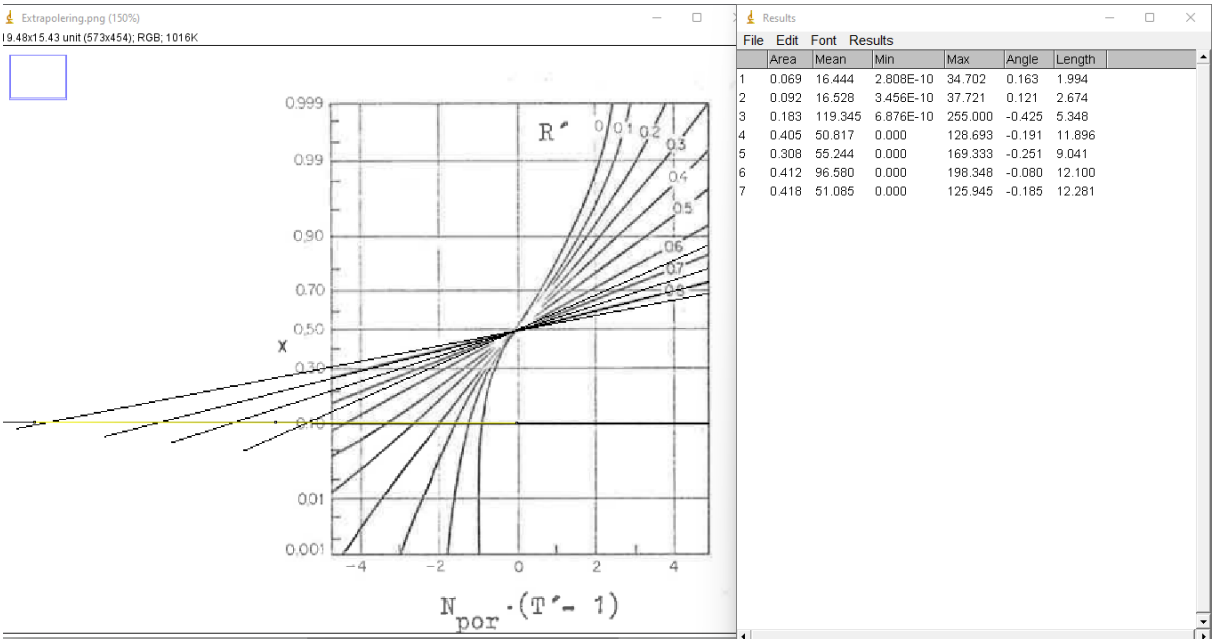

Figure 4: Extrapolated from Adsorptionsanläggningar (1977). Disregard 1st and 3rd measurements.

$$D_{pore} = \frac{D_c}{d_c^2} \cdot \lambda \cdot d_p^2$$

$$G_{sep,pore} = 0.452 \cdot \sqrt{R'}$$

$$\psi_{pore} = \frac{0.548}{1 - G_{sep}}$$

$$k_e \cdot a_p = \psi_{pore} \cdot k_{pore} \cdot a_p = \psi_{pore} \cdot \frac{10 \cdot D_{pore}}{d_p} \cdot a_p$$

$$N_{pore} = k_e \cdot a_p \cdot \frac{\theta_{ads}}{\epsilon} = k_{pore} \cdot a_p \cdot \frac{\theta_{ads}}{\epsilon}$$

$$N_{pore} \cdot (T'_{pore} - 1) = -\{Length\} \rightarrow$$

$$T'_{pore} = \frac{-\{Length\}}{N_{pore}} + 1$$

A.3.5. Basis for Choice of Model for Calculating the Breakthrough Times

$$\xi = \left(\frac{1}{k_f} + \frac{1}{k_d}\right) \cdot \left(\psi_{pore} \cdot k_{pore} + \psi_p \cdot \lambda \cdot k_p\right)$$

Since all $\xi > 1$, the media side (dispersion, outer mass transport) is determining the rate of adsorption, rather than the particle side (diffusion in the solid phase).

Since N_d (= 487.8047) > N_f (= 0.2060), the dispersion model is chosen to determine the breakthrough times.

A.3.6. Breakthrough Times Calculations

$$N = N_d + N_f$$

T’ dispersion model:

$$T' = \frac{\left[\frac{1}{1-R'} \cdot ln\frac{1}{1-X} + \frac{R'}{1-R'} \cdot lnX - \delta_d\right]}{N} + 1$$

$$\hat{t} = \frac{\rho_B \cdot q_0 \cdot \theta}{\epsilon \cdot c_0} \cdot T' + \theta$$

A.4. Thermal Regeneration

For multiple answers, the VOCs are listed in order:

Toluene - Acetone - MEK - n-Heptane - n-Octane

A.4.1. Set/Calculated General Dimensions and Variables with Constants Found in Literature

$C_{pads} = [1628.0 \quad 1549.6 \quad 1664.1 \quad 2145.5 \quad 2319.9]\ [J/(kg \cdot K)]$

$C_{pf} = 1003\ [J/(kg \cdot K)]$

$C_{ps}(T) = 2.58 \cdot T_2 + 704.90\ [J/(kg \cdot K)]$ (Qiu, 2000)

$C_{pst} = 502\ [J/(kg \cdot K)]$

$f_{ht} = 1.25$

$\Delta H_{vap} = 10^3 \cdot [35 \quad 31.3 \quad 33.5 \quad 34.5 \quad 37.5]\ [J/mole]$

$T_1 = 20\ [°C]$

$T_2 = 200\ [°C]$

$V_{0,reg} = 0.60\ [m/s]$

$H_f = 10^3 \cdot [1.005 \cdot T_2 + x_{moist} \cdot (1.88 \cdot T_2 + 2501)]$

$x_{moist} = 0$

$\xi = 1.0$ (for spheres)

$\rho_S = 7500\ [kg]$

A.4.2. Regeneration Times

$$\Delta T = T_2 - T_1$$

$$V_{reg} = \frac{V_{0,reg}}{\epsilon}$$

$$\theta_{reg} = \frac{x_2}{V_{reg}}$$

$m_{vol} = \frac{\pi}{4} \cdot [(D + 2 \cdot b)^2 - D^2] \cdot x_2$ (per adsorber)

$m_{st} = m_{vol} \cdot \rho_S$ (per adsorber)

$$j_h = 0.86 \cdot (Re)^{-0.41} \cdot \xi$$

$$h_f = j_h \cdot \left(\frac{C_{pf} \cdot \mu}{\varkappa}\right)^{-\frac{2}{3}} \cdot \left(C_{pf} \cdot V_{reg} \cdot \epsilon \cdot \rho_A\right)$$

$$h_s = \left(4 \cdot d_p\right)^{-1}$$

$$h_t = \left[\frac{1}{h_s} + \frac{1}{h_f}\right]^{-1}$$

$$n_{VOC} = \frac{\dot{Q}_{ads} \cdot c_{0,mg} \cdot 10^{-3} \cdot \hat{t}}{M_w}$$

$$\Delta H_{ads} \approx -\Delta H_{vap} \cdot n_{VOC}$$

$AX = \frac{h_t \cdot \theta_{reg} \cdot a_p}{C_{pf} \cdot \rho_A \cdot \epsilon} \rightarrow T_s' = \{Table\ value\}$ (Karlsson, 1977)

The three terms within the brackets in the equation below represent in order: heating of the bed, heating of the adsorber and adsorbate, and desorption. Since the enthalpy of adsorption ΔH_{ads} is negative, all terms add positive to the regeneration time t_s.

$$t_s = \theta_{reg} \cdot \left[\frac{\rho_B \cdot C_{ps} \cdot \Delta T}{\rho_A \cdot H_f} \cdot T_s' + \frac{\left(m_{st} \cdot C_{pst} + m_{ads} \cdot C_{pads}\right) \cdot \Delta T}{A \cdot x_2 \cdot \epsilon \cdot \rho_A \cdot H_f} - \frac{\Delta H_{ads}}{\rho_A \cdot H_f \cdot A \cdot x_2 \cdot \varepsilon}\right] \cdot f_{ht}$$

A.5. Catalytic combustion

For multiple answers, the VOCs are listed in order:

Toluene - Acetone - MEK - n-Heptane - n-Octane

A.5.1. Set/Calculated General Dimensions and Variables with Constants Found in Literature

$T_{ad} = [2344\ 2253\ 2300\ 2469\ 2290]\ [K]$

$n_C = [7\ 3\ 4\ 7\ 8]\ [Carbon\ atoms\ per\ molecule\ and\ specimen]$

$n_H = [8\ 6\ 8\ 16\ 18]\ [Hydrogen\ atoms\ per\ molecule\ and\ specimen]$

$n_O = [0\ 1\ 1\ 0\ 0]\ [Oxygen\ atoms\ per\ molecule\ and\ specimen]$

$$n_{O2,\Phi=1} = \frac{2 \cdot n_C + 0.5 \cdot n_H - n_O}{2}$$

$M_{O2} = 32\ [g/mol]$

$M_{N2} = 28\ [g/mol]$

$M_A = 0.21 \cdot M_{O2} + 0.79 \cdot M_{N2}$

A.5.2. Equivalence Ratio

$$n_{O2,\Phi=1,tot} = n_{O2,\Phi=1} \cdot n_{VOC}$$

$$n_{Air,\Phi=1,tot} = \frac{n_{O2,\Phi=1,tot}}{0.21}$$

$$n_{Air,des,tot} = \frac{\dot{Q}_{reg} \cdot \rho_A}{M_A} \cdot t_{des}$$

$$\phi = \frac{n_{Air,\Phi=1,tot}}{n_{Air,des,tot}}$$

A.5.3. Combustion and Temperatures

$$T_{ad,rise} = \phi \cdot T_{ad}$$

$$T_{ad,cat} = T_{in,cat} + T_{ad,rise}$$

A.6. Heat Requirements

A.6.1. Set/Calculated General Dimensions and Variables with Constants Found in Literature

$h_1 = h_2 = 50\ [W/(m^2 \cdot K)]$

$\lambda_T = 15\ [W/(m \cdot K)]$

$L_T = 0.002\ [m]$

A.6.2. Heat and Area Requirements

$$U = \left[\frac{1}{h_1} + \frac{L_T}{\lambda_T} + \frac{1}{h_2}\right]^{-1}$$

$$\Delta T_{L,1} = T_{ad,cat} - T_2$$

$$\Delta T_{L,2} = T_{out,cat} - T_1$$

$$\Delta T_L = \frac{\Delta T_{L,1} - \Delta T_{L,2}}{ln\left(\frac{\Delta T_{L,1}}{\Delta T_{L,2}}\right)}$$

$$Q = C_{pf} \cdot \dot{Q}_{reg} \cdot \rho_A \cdot (T_2 - T_1) = C_{pf} \cdot \dot{Q}_{reg} \cdot \rho_A \cdot \left(T_{ad,cat} - T_{in,cat}\right) = U \cdot A_T \cdot \Delta T_L \rightarrow$$

$$A_T = \frac{C_{pf} \cdot \dot{Q}_{reg} \cdot \rho_A \cdot (T_2 - T_1)}{U \cdot \Delta T_L} = \frac{C_{pf} \cdot \dot{Q}_{reg} \cdot \rho_A \cdot \left(T_{ad,cat} - T_{in,cat}\right)}{U \cdot \Delta T_L}$$

$$\Delta T_{L,1} = \Delta T_{L,2} \rightarrow \Delta T_L = \Delta T_{L,1} = \Delta T_{L,2} = T_2 - T_1 = T_{ad,cat} - T_{in,cat} \rightarrow$$

$$A_T = \frac{C_{pf} \cdot \dot{Q}_{reg} \cdot \rho_A}{U}$$

A.7. Annuity Costs and Depreciation

A.7.1 Set/Calculated General Dimensions and Variables with Constants Found in Literature

$x_{int} = 0.05$

$N_Y = 25\ [years]$

$f_{MnR} = 0.06$

$f_{Spare} = 0.15$

$Total\ Module\ Cost = 12\ 810\ 080\ [SEK]$

$Grass\ Roots\ Capital = 17\ 218\ 300\ [SEK]$

A.7.2. Annuity Costs Equations

$$f_A = \frac{x_{int}}{(1-(1+x_{int})^{-N_Y})}$$

$$MnR_{Annual} = f_A \cdot f_{MnR} \cdot [Grass\ Roots\ Capital]$$

$$Spare_{Annual} = f_A \cdot f_{MnR} \cdot f_{Spare} \cdot [Grass\ Roots\ Capital]$$

A.7.3. Depreciation

$$[Depreciation] = \frac{[Total\ Module\ Cost]}{N_Y}$$